Supplementary Information

Ordered Mesoporous Carbon Nanochannel Reactors for High-Performance Fischer-Tropsch Synthesis

Kyoung-Su Ha[*a], Geunjae Kwak[a], Ki-Won Jun[a],

Jongkook Hwang[b], Jinwoo Lee[*b]

[a]*Korea Research Institute of Chemical Technology, 141 Gajeongro, Yuseong, Daejeon, Korea, 305-600*

[b]*POSTECH, 77 Cheongam-Ro, Nam-Gu, Pohang, Gyungbuk, Korea, 790-784*

Keywords: : cobalt · Fischer-Tropsch catalyst · hydrogenation · nano-channel reactor · ordered mesoporous carbon

* To whom all correspondence should be addressed. Tel.: (+82)-42-860-7286, Fax: (+82)-42-860-7388, E-mail: filoseus@krict.re.kr .

Tel.:(+82)-54-279-2395, Fax: (+82)-42-860-7388, E-mail:jinwoo03@postech.ac.kr.

Section S1. The properties of carbon support and the chemical treatment of its surface

The carbon material is known to be rather inert to active catalytic materials.[S1] This feature is of great importance to FTS since the strong interaction between catalytic material and support material can cause to oxidize metal, which leads to loss of activity and selectivity. In this study, we used the treatment with diluted nitric acid solution (1M) to form slight amount of hydrophilic functionalities enough to infiltrate the cobalt precursors inside the mesopores[S1] but the treatment was so weak that the structure was not influenced as shown in Figs. S2 & S3, and most of the surface remained hydrophobic, which is shown in Fig. S10. Therefore, the carbon surface after mild treatment was barely affected and most of part remained hydrophobic. As far as the heat transfer is concerned, the thermal conductivity of carbon material is so high that it can promptly dissipate the heat of very exothermic reaction (-165 kJ/CO mol).[S2] The thermal conductivity ranges from 120-165 W/m·K, which is about 4 times and about 100 times greater than those of alumina and silica, respectively. According to Russell,[S3] the effective thermal conductivity of porous medium can be expressed as Eqn 1.

$$k_{eff} = k_{solid} \times [\varepsilon^{2/3} k_{fluid} + k_{solid} (1- \varepsilon^{2/3})]/[k_{fluid} (\varepsilon^{2/3} - \varepsilon) + k_{solid} (1- \varepsilon^{2/3} + \varepsilon)] \qquad \text{(Eqn 1)}$$

where, k_{eff}, k_{fluid}, k_{solid} and ε represent the effective thermal conductivity, the fluid thermal conductivity, the catalyst thermal conductivity and the porosity of catalyst bed, respectively. The Eqn 1 shows that k_{eff} has proportional relationship with k_{solid}. Therefore, the heat transfer rate at the catalyst bed can be enhanced if we employ a support with high thermal conductivity such as carbon materials.

Section S2. Catalyst characterization: BET, TPR, XRD, XPS, FT-IR, TEM, and H_2-chemisorption methods.

The surface area, pore volume and pore size distribution of FTS catalysts (or supports) were estimated from nitrogen adsorption method obtained at −196 ℃ using a constant-volume adsorption apparatus (Micromeritics, ASAP-2400). The calcined catalysts (or supports) were previously degassed at 300 ℃ in a He flow for 4 h before the measurements. The pore volume was determined at a relative pressure (P/Po) of 0.99. Pore size distribution of the catalysts was calculated using the BJH (Barett–Joyner–Halenda) model from the data of desorption branch of the nitrogen isotherms.

The temperature-programmed reduction (TPR) experiment was performed to determine the reducibility of Co_3O_4 particles. Prior to TPR experiment, the catalyst was pretreated in a He flow up to 350 ℃ and kept for 2 h to remove the adsorbed water and other contaminants followed by cooling to 50 ℃. The reducing gas containing 5% H_2/He mixture was passed over the samples at a flow rate of 30 ml/min with a heating rate of 10 ℃/min up to 900 ℃. The effluent gas was passed over a molecular sieve trap to remove the water formed and analyzed by GC equipped with TCD.

The powder X-ray diffraction (XRD) patterns of FTS catalysts were obtained with a Rigaku diffractometer using Cu-Kα radiation to identify the crystalline phases of cobalt particles and to determine the particle size of Co_3O_4 and metallic cobalt together.

Small-angle X-ray scattering (SAXS) experiments were carried out on the 4C SAXS beamline at the Pohang Light Source (PLS). The beamline was equipped with an in-vacuum undulater 20 (IVU 20) and Rayonix 2D SX165. X-rays with a wavelength of 1.24 A were used and sample-to-detector distance was 3 m.

The surface cobalt species, carbon species and their binding energies (BEs) of Co 2p and C 1s on the FTS catalyst were characterized by using X-ray photoelectron spectroscopy (XPS; ESCALAB MK-II) analysis. During the experiment, AlKα mono-chromatized line (1486.6 eV) was adopted and the vacuum level was kept around 10^{-7} Pa. The used FTS catalyst without washing treatment was previously pressed to a thin pellet and the binding energy (BE) was corrected with the reference BE of C1s (284.4 eV).

The in situ diffuse reflectance infrared Fourier transform (DRIFT) analysis of the adsorbed H_2O molecule on FTS catalyst was performed with Nicolet 6700 equipped with MCT detector which was cooled with liquid nitrogen and had a spectral resolution of 4 cm^{-1}. After the power catalyst samples were placed into a cell and reduced with 99.999% H_2 flowing at 400 ℃ for 6 h. They were cooled down to 50 ℃ followed by purging with He for 30 min and the background spectra were measured. Adsorption of H_2O was conducted by flowing He gas with saturated H_2O at 50 ℃ for 30 min followed by purging with dry He gas for 10 min to remove physisorbed H_2O molecules before FT-IR measurement. The spectra were provided after subtraction of their background spectra.

The surface morphology and the cobalt particle for the catalysts were characterized by using JEOL JEM-ARM200F operating at 200 kV. Nano structures of the catalysts were analyzed by HR-TEM, and the elemental analysis was conducted with the help of EDX method using Bruker Quantax 400.

The dispersion and the cobalt particle size were calculated from H_2-chemisorption method at 100 ℃ under static condition using a Micrometrics ASAP 2020C. Prior to adsorption experiments, the catalysts were reduced at 400 ℃ for 12 h in a H_2 flow at SV = 6000 ml/g_{cat}/h. The metal dispersion was calculated with the assumption of H/Co stoichiometry of 1. The DR was determined by O_2-titration method and then the particle size of Co was obtained by considering the DR and the dispersion. After measurement or estimation of Co^0 crystal size, dispersion was calculated by $96.2/d(Co^0)$

Section S3. Estimation of the size of Co^0 from the size of CoO crystal.

CoO crystals adopt the rock salt structure with a lattice constant of 4.2615 Å.[S4] In the unit crystal, there are 4 Co atoms and 4 O atoms in it. And the covalent radius of Co can be estimated as 1.35 Å considering low spin and high spin cases.[S5] Then, the volume fraction and of Co atoms and the estimated size of Co^0, $d(Co^0)$, can be properly computed as follows;

The volume ratio of Co atoms = $4 \times (4\pi/3 \cdot (1.353\ \text{Å})^3) / (4.2615\ \text{Å})^3 = 0.532$.

The estimated size Co^0, $d(Co^0) = (0.532)^{(1/3)} \times d(CoO) = 0.810 \times d(CoO)$.

The $d(Co^0)$ can be calculated from Co_3O_4 crystal as follows; [S6]

The estimated size Co^0, $d(Co^0) = 0.75 \times d(Co_3O_4)$.

S4. Experimental Section

After pre-treatment (see the Supplementary Information, Section S1), the appropriate amount of cobalt precursor ($Co(NO_3)_2 \cdot 6H_2O$) was successfully infiltrated into the carbon mesopores of CMK-3 and MUS-F-C during incipient wetness impregnation (IWI). After drying at 110 ℃ for 12 h, cobalt impregnated carbon material was calcined at 400 ℃ under N_2 flowing condition for 5h. Unlike the calcination under air-flowing condition, the cobalt oxide phase was primarily obtained in the form of CoO, instead of Co_3O_4 (Fig. S7). The 20Co/γ-Al_2O_3 with 20 wt.% Co on γ-Al_2O_3 support (surface area of 170 m^2/g, Puralox^{TM}) was prepared by IWI method with the cobalt precursor, ($Co(NO_3)_2 \cdot 6H_2O$). After impregnation, it was dried at 110 °C for 12 h, and calcined at 400 °C for 5h. After calcination, the prepared catalysts were evaluated in a micro fixed-bed reactor. The 0.3 g catalysts with 1.5 g α-Al_2O_3 were previously reduced in situ at 400 ℃ for 12 h flowing 5% H_2/He reduction gas mixture at SV= 5000 mL/g_{cat}/h. A series of FTS runs were conducted in a micro fixed bed reactor at GHSV = 4000 syngas ml/g-cat/h, P = 2.0 MPa, T = 220 ℃, H_2/CO ratio = 2.0. Syngas composition is $H_2/CO/CO_2/Ar$ = 57.3/28.4/9.3/5.0 (mol %). The effluent gas from the reactor was analyzed by an online gas chromatograph (YoungLin Acme 6000 GC) employing GS-GASPRO capillary column connected with a flame ionization detector and a Porapack Q/molecular sieve (5A) packed column connected with a thermal conductivity detect. Ar was used as an internal standard for GC analysis. The conversion was computed based on CO consumption and the selectivity was calculated on a carbon mole basis. BET, TPR, XRD, XPS, FT-IR and TEM methods were employed to characterize the Fischer-Tropsch catalysts (see the Supplementary Information, Section S2). For the observation in Fig. S4, the catalysts were reduced as mentioned above and passivated by flowing 1% O_2/N_2 (balance) gas mixture for 1 h after cooling down to room temperature.

Table S1. H_2-Chemisorption and O_2-titration result of 20Co/γ-Al_2O_3 catalyst.

catalyst	H_2 Chemisorption				O_2 consumption	Degree of reduction (%) [b)]
	H_2 uptake (μmol/g)	Dispersion (%) [a)]	Uncorrected size (nm)	Corrected size (nm) [b)]	(μmol/g)	
20Co/γ-Al_2O_3	71.9	6.0	23.5	16.0	1597.7	70.6

[a)] The dispersion and cobalt particle size were calculated from H_2 chemisorption and it was corrected by considering the degree of reduction.[S7]

[b)] The reduction degree (%) was calculated from the amount of O_2 consumption divided by the theoretical O_2 consumption by the equation of $3Co + 2O_2 \rightarrow Co_3O_4$.

Table S2. Crystal sizes of CoO, Co_3O_4, and Co^0 from XRD and lattice structure.

Catalyst	Particle size from XRD [a] (nm)	Particle size of Co^{0} [b] (nm)	% Dispersion 96.2/*d*(Co^0) [S7]
20Co@CMK-3	4.0 (CoO)	3.2	30.1
20Co/MSU-F-C	8.7 (CoO)	7.0	11.1
20Co/γ-Al_2O_3	14.4 (Co_3O_4)	10.8	8.9

[a] Calculated by Scherrer's formula[S8] in Fig. S7 at a Bragg angle (2θ) of 43.1° for CoO. The size of Co_3O_4 crystal was calculated at a 2θ of 36.8°.

[b] Estimated by methods in Section S3 (Supplementary Information).

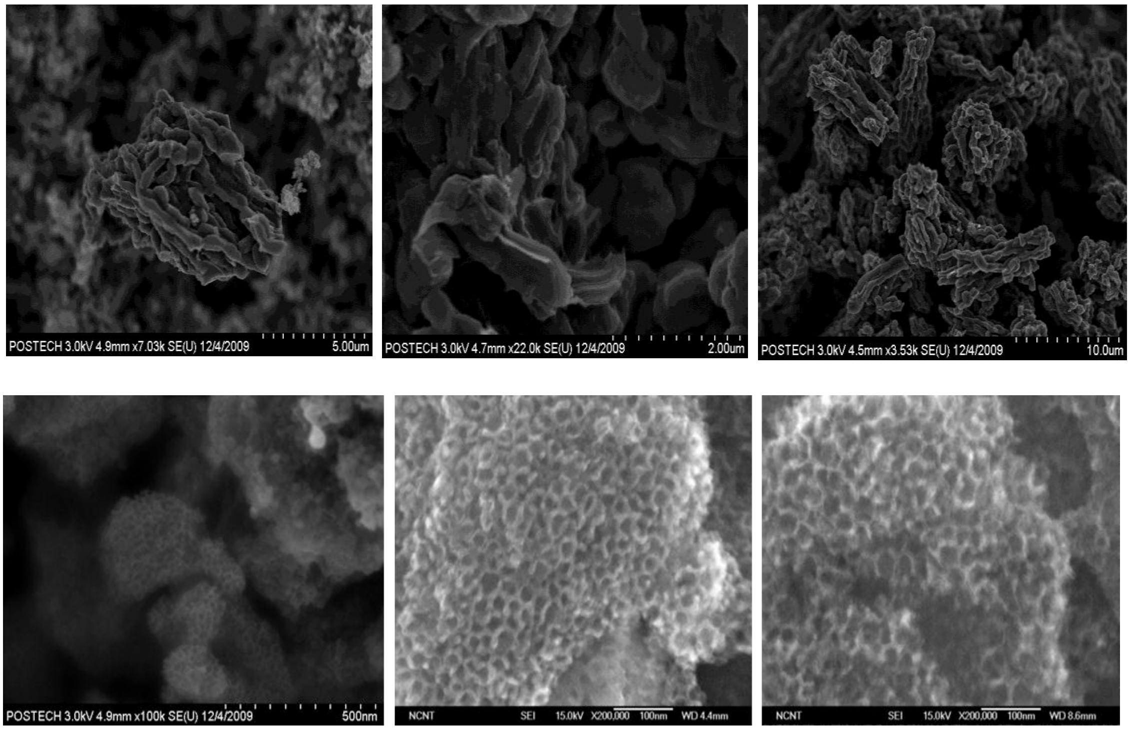

Fig. S1. SEM images of CMK-3 (top) and MSU-F-C (bottom).

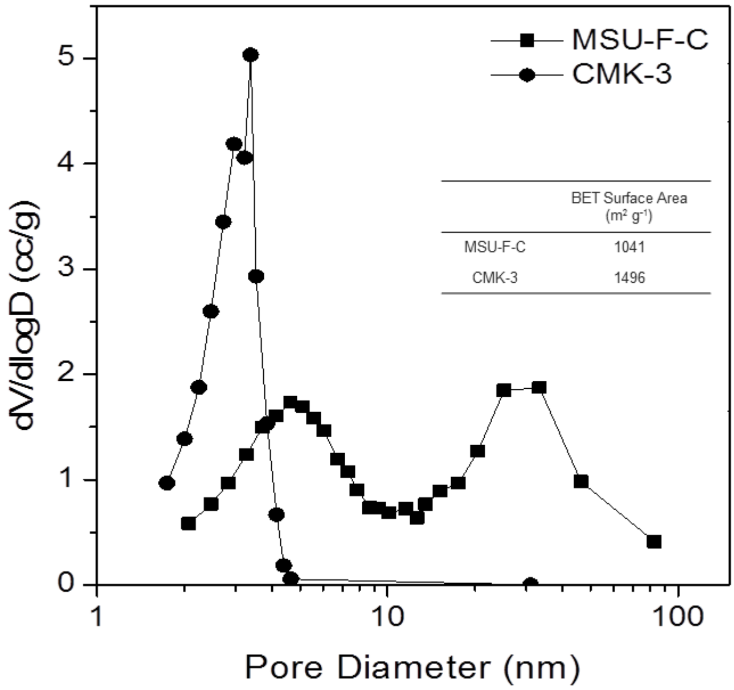

	BET Surface Area (m² g⁻¹)
MSU-F-C	1041
CMK-3	1496

Fig. S2. Surface areas and the pore size distributions after HNO_3 treatment by BET and BJH (Barett–Joyner–Halenda) methods, respectively.

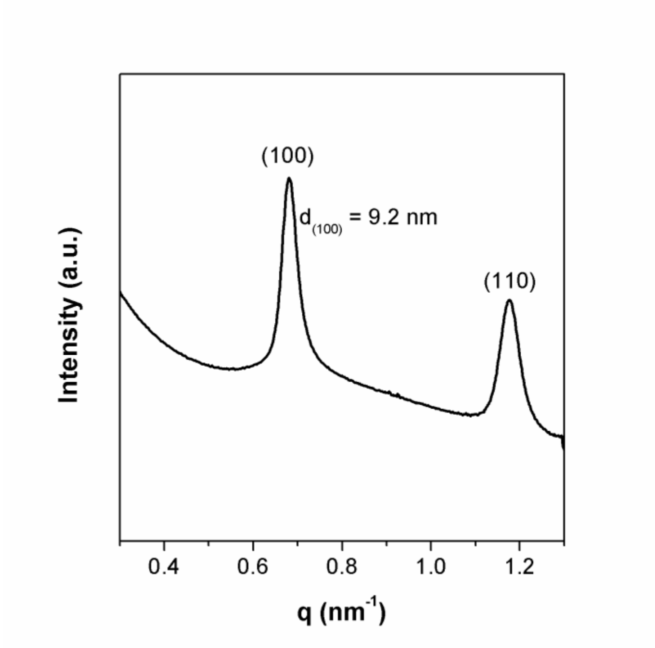

Fig. S3. Small angle X-ray scattering pattern of CMK-3 after HNO_3 treatment. (100) and (110) peaks for typical 2-D hexagonal structure (space group p6mm) are shown in this pattern.

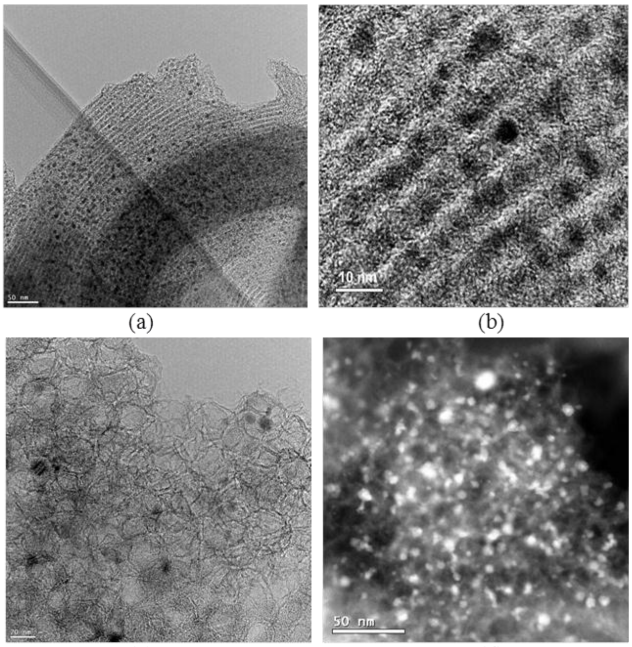

(a) (b) (c) (d)

Fig. S4. TEM images after reduction and passivation; (a) 20Co@CMK-3, scale bar = 50 nm; (b) 20Co@CMK-3, scale bar = 10 nm; (c) 20Co/MSU-F-C, scale bar = 20 nm; (d) 20Co/MSU-F-C, scale bar = 50 nm.

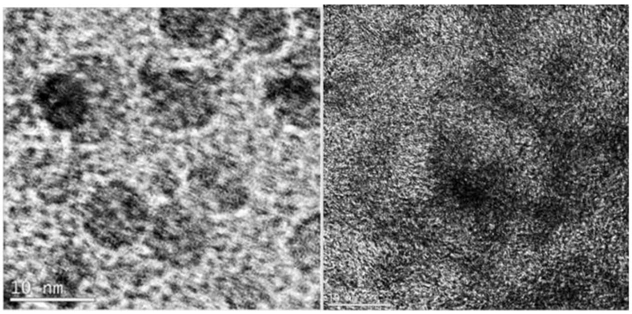

(a) (b)

Fig. S5. TEM images of (a) 20Co@CMK-3 and (b) 20Co/MSU-F-C after 40 h Fischer-Tropsch synthesis reaction. Each scale bar denotes 10 nm.

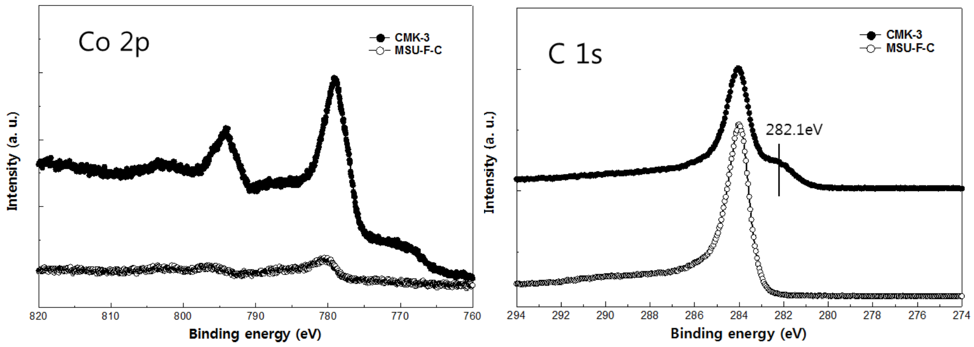

(a) (b)

Fig. S6. XPS results of CMK-3 and MSU-F-C supported cobalt catalyst (calcined) ; (a) Co $2p_{3/2}$ and Co $2p_{1/2}$ photoelectron peak of nano CoO crystals with CMK-3 and MSU-F-C ; (b) C 1s photoelectron peak of nano CoO crystals with CMK-3 and MSU-F-C.

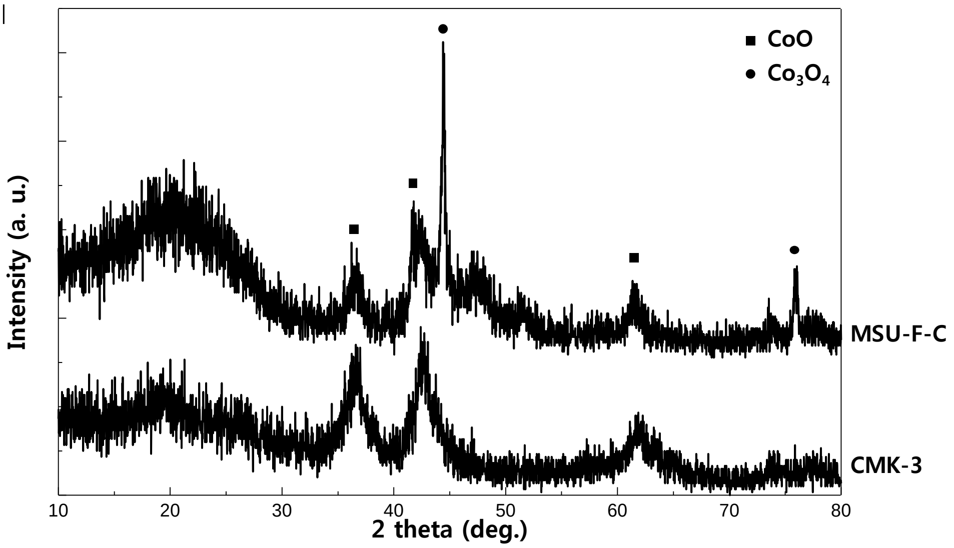

Fig. S7. XRD patterns of mesoporous carbon supported Co catalysts (calcined); Solid Squares and solid circles indicated CoO and Co_3O_4 crystals, respectively. In the case of Co@CMK-3 support, clean CoO crystals were obtained whereas Co/MSU-F-C was found to have a slight amount of Co_3O_4.

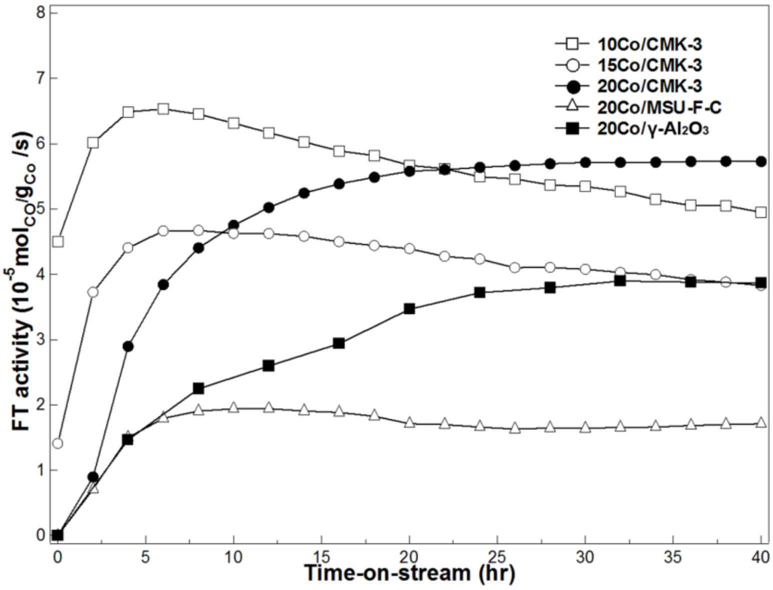

Fig. S8. FT activity profiles of alumina and mesoporous carbon-supported cobalt catalysts with time on stream.

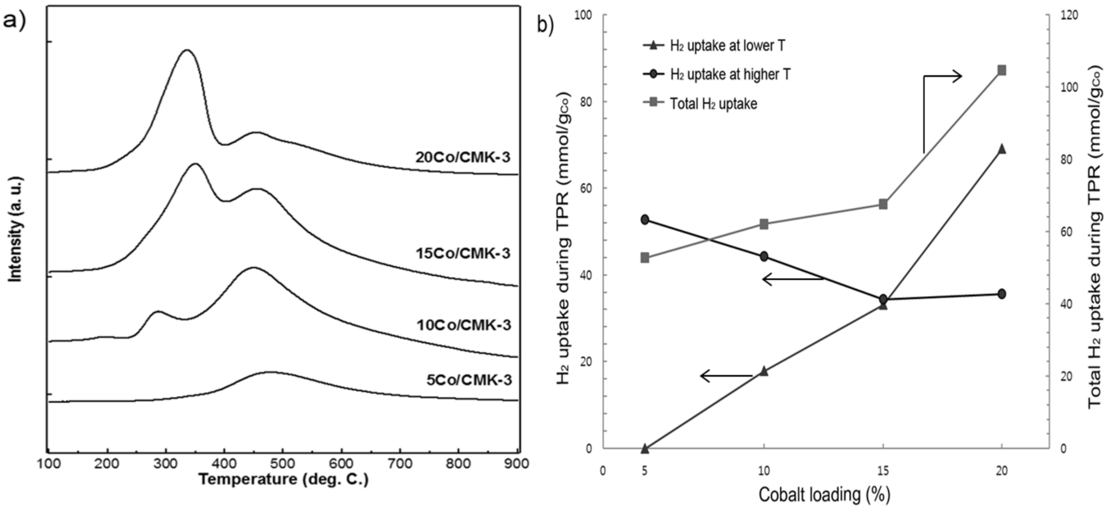

Fig. S9. TPR profiles for Co@CMK-3 with various cobalt loadings; (a) TPR profiles; (b) H_2 uptake (mmol/g_{Co}) profiles for lower temperature reduction peaks from 150 to 350℃, for higher temperature reduction peaks from 350 to 900 ℃, and for the entire temperature range.

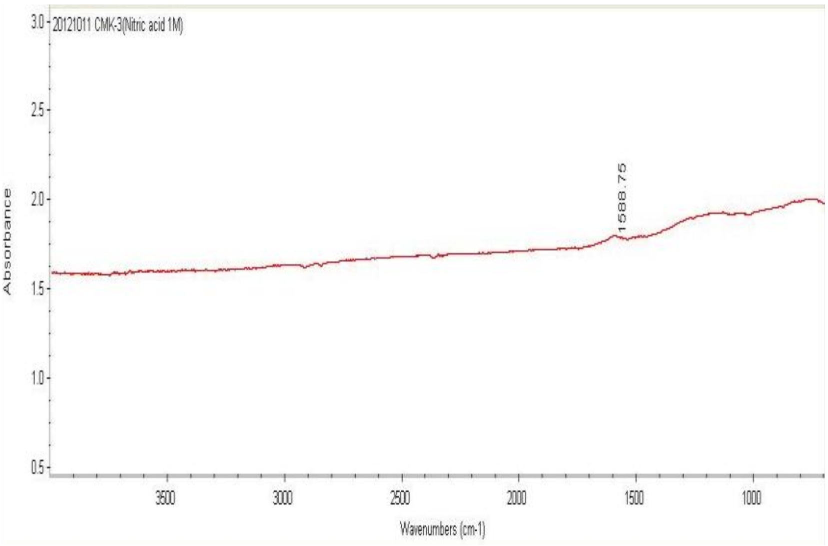

Fig. S10. The FT-IR spectrum of 1M HNO_3 solution-treated CMK-3 surface.

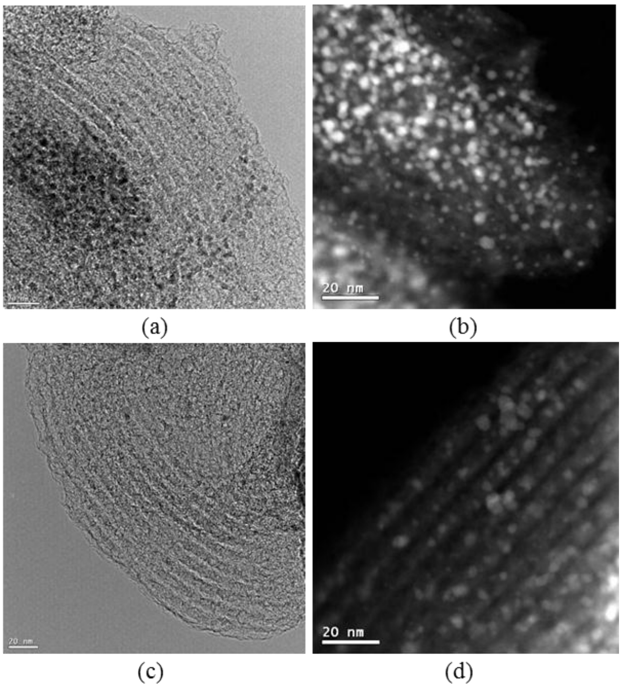

(a) (b)

(c) (d)

Fig. S11. TEM images of CMK-3-supported NCR (calcined) with different loadings of Co. (a) and (b) 15Co@CMK-3, scale bar = 20 nm; (c) and (d) 10Co@CMK-3, scale bar = 20 nm.

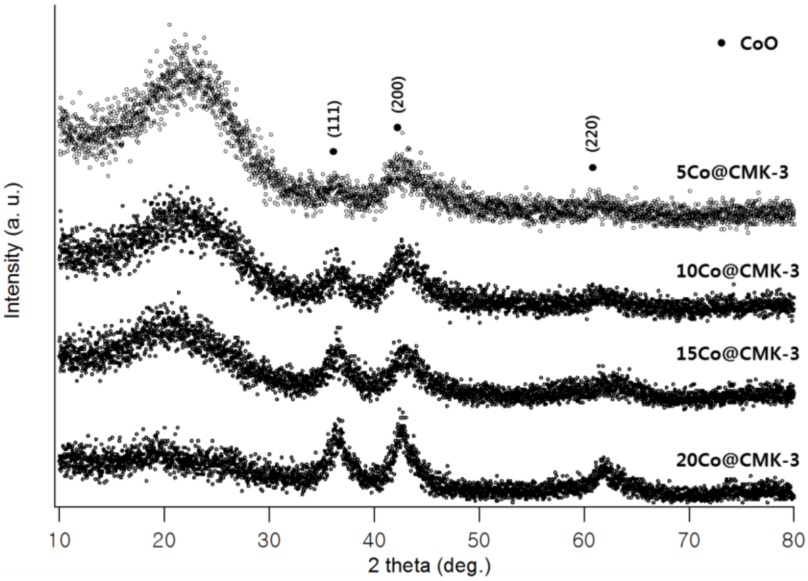

Fig. S12. XRD data of 20Co@CMK-3, 15Co@CMK-3, 10Co@CMK-3 and 5Co@CMK-3 (calcined).

REFERENCES

S1 a) G. L. Bezemer, J. H. Bitter, H. P. C. E. Kuipers, H. Oosterbeek, J. E. Holewijn, X. Xu, F. Kapteijn, A. J. van Dillen, K. P. de Jong, *J. Am. Chem. Soc*., 2006, **128**, 3956; b) V. Papaefthimiou, T. Dintzer, V. Dupuis, A. Tamion, F. Tournus, A. Hillion, D. Teschner, M. Hävecker, A. Knop-Gericke, R. Schlőgl, S. Zafeiratos, *ACS Nano*, 2011, **5**, 2182.
S2 M. Sheng, H. Yang, D. R. Cahela, B. J. Tatarchuk, *J. Catal*, 2011, **281**, 254.
S3 H.W.Russell, *J. Am. Ceram. Soc.* 1935, **18**, 1.
S4 R. Kannan, S. S. Mohindar, *Phys. Rev. B*, 1987, **35**, 6847.
S5 J. C. Slater, *J. Chem. Phys*, 1964, **41**, 3199.
S6 D. Schanke, S. Vada, E. A. Blekkan, A. M. Hilmen, A. Hoff, A. Holmen, *J. Catal.*, 1995, **156**, 85.
S7 R.D. Jones, C.H. Bartholomew, *Appl. Catal.*, 1988, **39**, 77.
S8 A. L. Patterson, *Phys. Rev.*, 1939, **56**, 978.